

Electronic Supplementary Information

10 May, 2020

Ms. ID: NR-ART-04-2020-002929

**Multilayer electrodeposition of Pt onto 1-2 nm Au nanoparticles
using a hydride-termination approach**

Aliya S. Lapp and Richard M. Crooks

Table of Contents

Page

S2	The rate of change in Pt coverage as a function of the number of HT pulses
S2	Pt and Au electrochemically active surface areas
S3	Theoretically predicted electrochemical, TEM and XPS parameters
S4	Comparison of the calculated number of Pt MLs determined from XPS and electrochemical analysis
S4	Plot of the theoretical Pt and Au compositions for an ideal cuboctahedral Au ₁₄₇ NP with 1 to 10 ML of deposited Pt
S5	EDS line profiles for an AuPt NP prepared using 10 HT pulses
S6-10	EDS for AuPt DENs prepared using 1 to 5 HT pulses
S11	Electrochemical surface characterization after 20 FAO cycles
S12	Comparison of FAO results for the forward-going scans of the first and 20 th FAO CVs
S13	References

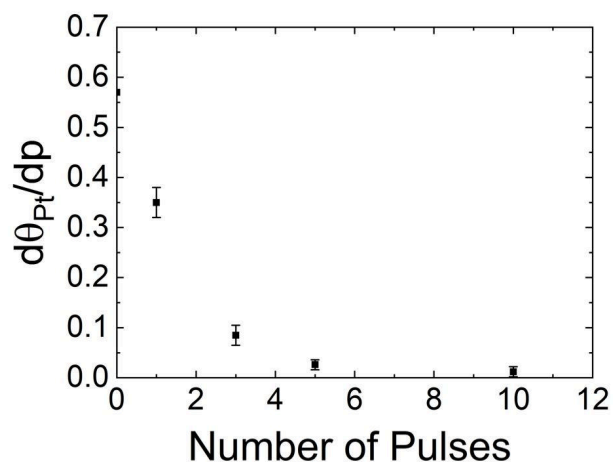


Figure S1. The rate of change ($d\theta_{Pt}/dp$) in Pt coverage (θ_{Pt}) as a function of the number of HT pulses. The rate of change approaches zero after 5 HT pulses.

Table S1. Pt and Au electrochemically active surface areas (ECSAs), as a function of the number of HT pulses. The Au_i ECSA corresponds to the ECSA of the naked Au_{147} NP surface (prior to HT Pt deposition). The Au_f ECSA is the remaining Au ECSA after HT Pt deposition. In each case, the area under the AuO_x reduction peak was integrated and the resulting charge was converted to ECSA using the charge density for polycrystalline Au ($390 \mu C/cm^2$).¹ Pt ECSA determination used the same procedure, except the Pt-H adsorption waves were integrated and the charge density for polycrystalline Pt ($210 \mu C/cm^2$)¹ was used to convert charge to ECSA. $ECSA_{tot}$ is the total NP ECSA (= Au_f ECSA + Pt ECSA).

Pulses	Au_i ECSA (cm^2)	Au_f ECSA (cm^2)	Pt ECSA (cm^2)	$ECSA_{tot}$ (cm^2)
1	0.260(9)	0.11(1)	0.160(7)	0.27(1)
3	0.25(3)	0.041(2)	0.31(4)	0.36(4)
5	0.26(4)	0.022(4)	0.48(8)	0.50(8)
10	0.28(3)	0.007(3)	0.74(8)	0.75(8)

Table S2. Theoretically predicted electrochemical, TEM, and XPS parameters for the deposition of 1 to 4 monolayers (MLs) of Pt onto a cuboctahedral Au₁₄₇ NP. N_{surf} is the number of surface atoms (Au + Pt), Pt:Au_i is the ideal electrochemical Pt:Au_i ECSA ratio, d is the theoretically predicted NP diameter, N_{tot} is the total number of atoms (core + shell(s)) in each NP, $N_{Pt,tot}$ is the total number of Pt atoms in each NP, and atomic% Pt is the atomic Pt composition predicted for XPS. Pt:Au_i was calculated as N_{surf} in each layer divided by N_{surf} for 0 ML (corresponding to the number of surface atoms in the Au₁₄₇ core). The values of d were calculated using cuboctahedral cluster models from the Atomic Simulation Environment (ASE) Python library.² The diameter of each cluster model was measured using the ASE graphical user interface. $N_{Pt,tot}$ was calculated as the sum of N_{surf} in a given layer plus N_{surf} in the preceding layer(s) (e.g., 162+252=414 for 2 ML). The atomic% Pt values were calculated as $100\% * N_{Pt,tot} / N_{tot}$. An ideal core@shell Au₁₄₇@Pt model was assumed in all cases.

Layers	N_{surf}	Pt:Au _i	d (nm)	N_{tot}	$N_{Pt,tot}$	Atomic% Pt
0 ML	92	-	1.7	147	-	-
1 ML	162	1.8	2.3	309	162	52
2 ML	252	2.7	2.8	561	414	74
3 ML	362	3.9	3.4	923	776	84
4 ML	492	5.3	4.0	1415	1268	90

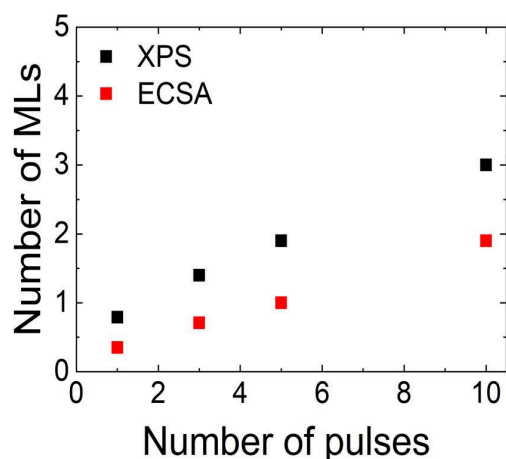


Figure S2. Comparison of the calculated number of Pt MLs determined from XPS and electrochemical analysis (ECSA), as a function of the number of HT pulses. For XPS, the number of Pt MLs was calculated by comparing the experimental atomic% Pt values (Figure 3b) to those theoretically calculated (Table S2 and Figure S3). Similarly, the number of MLs determined by electrochemistry was calculated by comparing the experimental Pt:Au_i ECSA ratios (Table 1) to the theoretical Pt:Au_i ECSA values (Table S2) for deposition of Pt on an ideal cuboctahedral Au₁₄₇ NP.

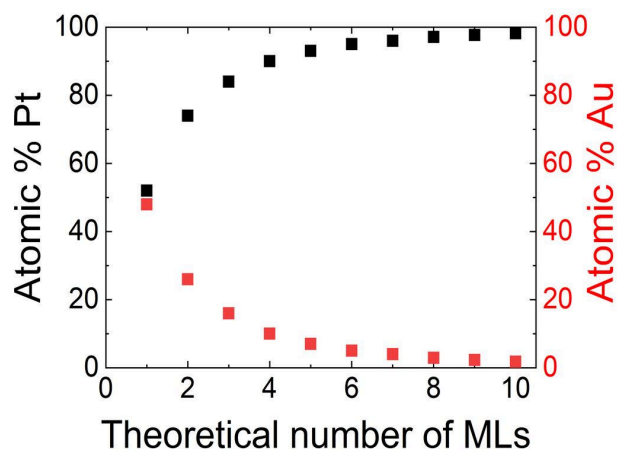


Figure S3. Plot of the theoretical Pt and Au compositions for an ideal cuboctahedral Au₁₄₇ NP with 1 to 10 ML of deposited Pt.

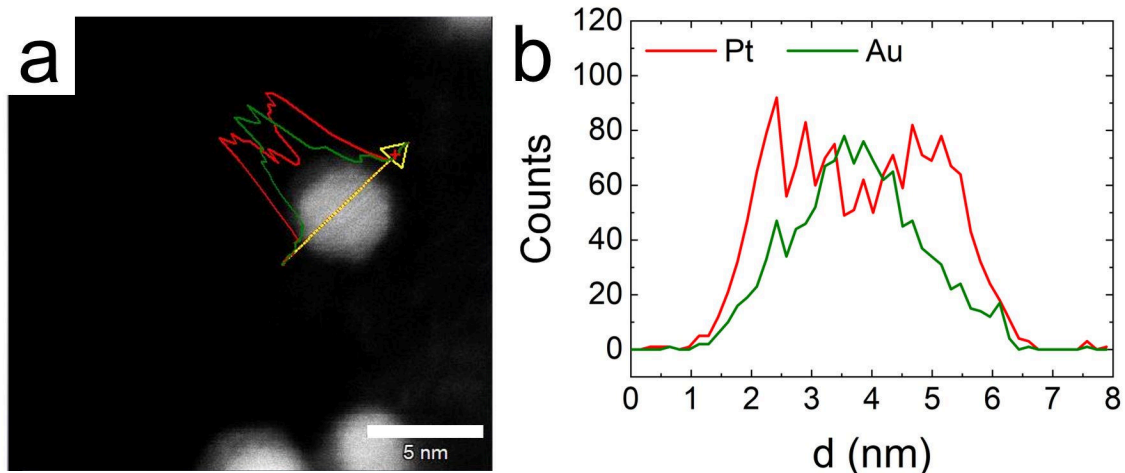


Figure S4. EDS line profiles for an AuPt NP prepared using 10 HT pulses (a) overlaid on the corresponding STEM micrograph and (b) a magnified view. This line scan was obtained directly (rather than being extracted from the map in Figure 4a). Line scan direction is indicated by the arrow in (a). As shown in (a), the line profile spans a distance that is larger than the NP. This might be due to drift during the line scan, as suggested by the larger gap between the NP and the line profile at the end of the scan (tip of the arrow) than at the beginning (arrow tail). Consequently, estimates of NP diameter and shell thickness using the x-axis in (b) are inaccurate. For example, although the diameter of the NP in the STEM micrograph corresponding to (a) is 4.2 nm, the line profile in (b) suggests NP size is between 5.2 and 5.8 nm (depending on where the baseline is drawn). Thus, the diameters in (b) are overestimated by ~1.0 to 1.6 nm. Accordingly, this line profile is only provided to highlight the core@shell structure of the NPs prepared using 10 HT pulses.

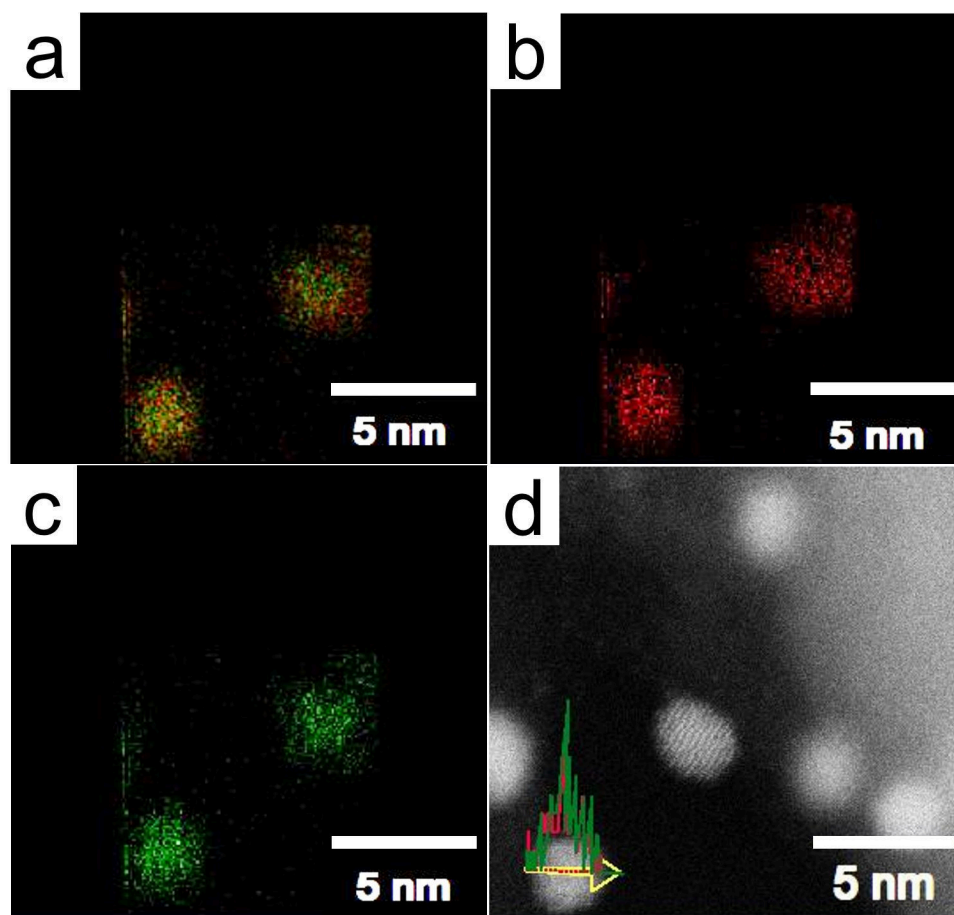


Figure S5. EDS for AuPt DENs prepared using 1 HT pulse. (a) Overlaid Pt (red) and Au (green) EDS maps. The NP on the lower left was stable during EDS measurements, but the NP on the right side of frame (a) may have been damaged by merging with a nearby NP during mapping. Individual (b) Pt and (c) Au maps corresponding to (a). (d) Line scan extracted from the map of the NP on the left side of frame (a) overlaid on the corresponding STEM micrograph.

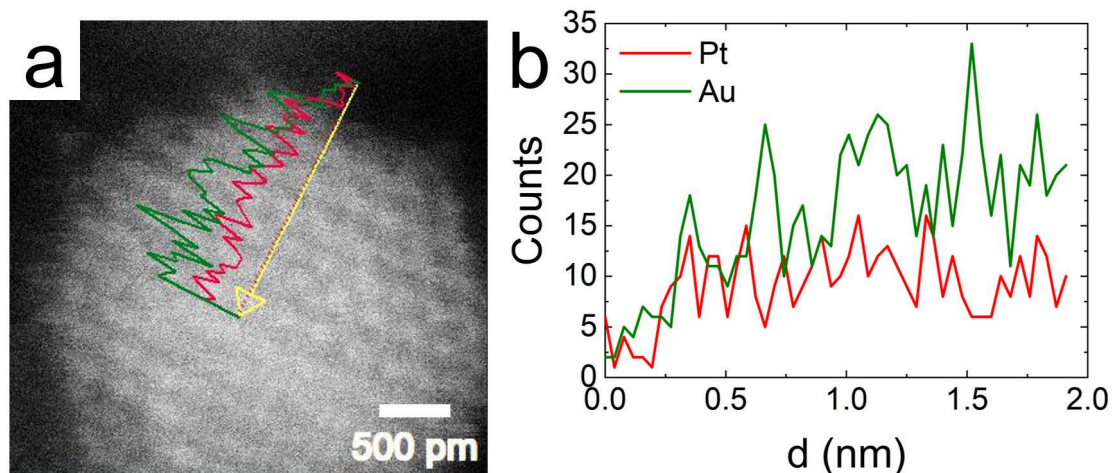


Figure S6. High-resolution line scan for AuPt DENs prepared using 1 HT pulse. (a) High-resolution, aberration-corrected STEM (acSTEM) micrograph, with EDS line scan overlaid. (b) Magnified view of the line scan in (a). Pt and Au may be alloyed in the outermost shell of the NP ($d \sim 0.3$ to 0.6 nm; 0 to 0.3 nm in this case is just noise). Beyond ~ 0.6 nm, the Au counts increase, whereas the Pt counts remain approximately constant. This result suggests that the alloying observed in the surface of the NP does not extend appreciably into the core. Therefore, the AuPt DENs prepared using 1 HT pulse are likely surface alloys. This finding is consistent with our previous report.³ We note, however, that the small number of counts, as well as the signal-to-noise ratio in (b), makes it difficult to draw firm conclusions.

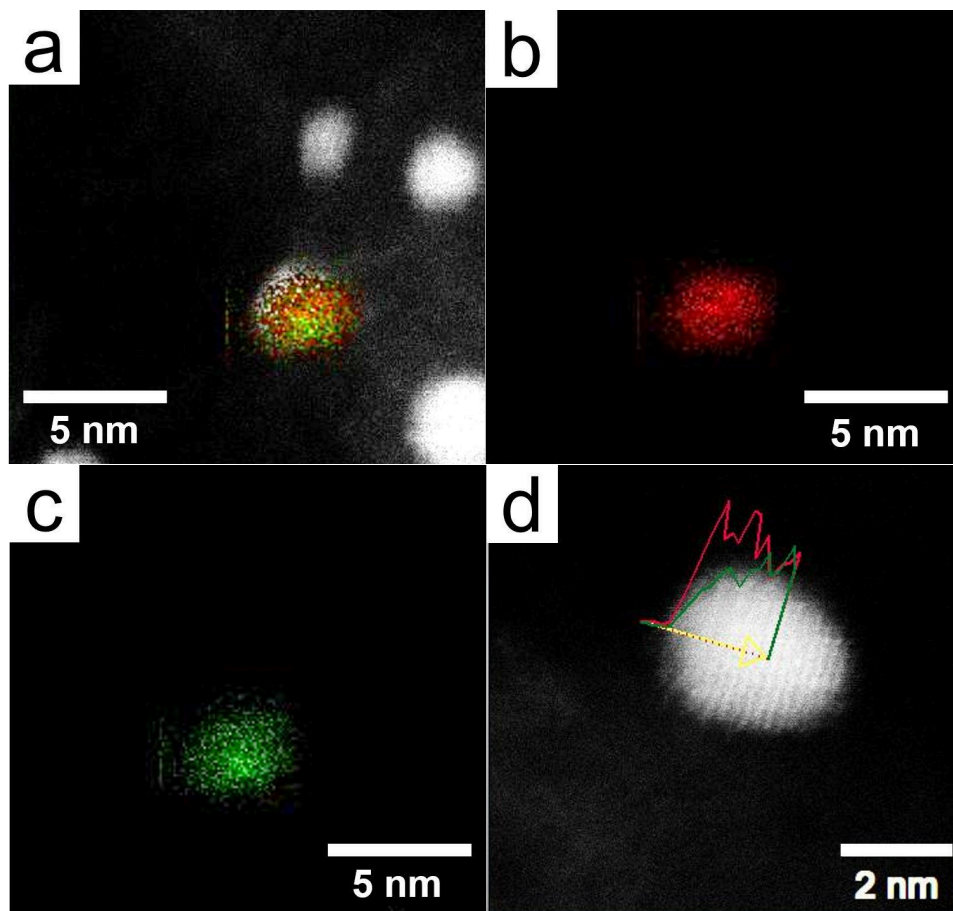


Figure S7. EDS for AuPt DENs prepared using 3 HT pulses. (a) Overlaid Pt (red) and Au (green) EDS maps. Individual (b) Pt and (c) Au maps for the combined map shown in (a). (d) acSTEM line scan of a representative NP. Pt is dominant in the first 0.3 nm of the NP, which corresponds to the outermost shell. Beyond 0.3 nm, Pt and Au are mixed.

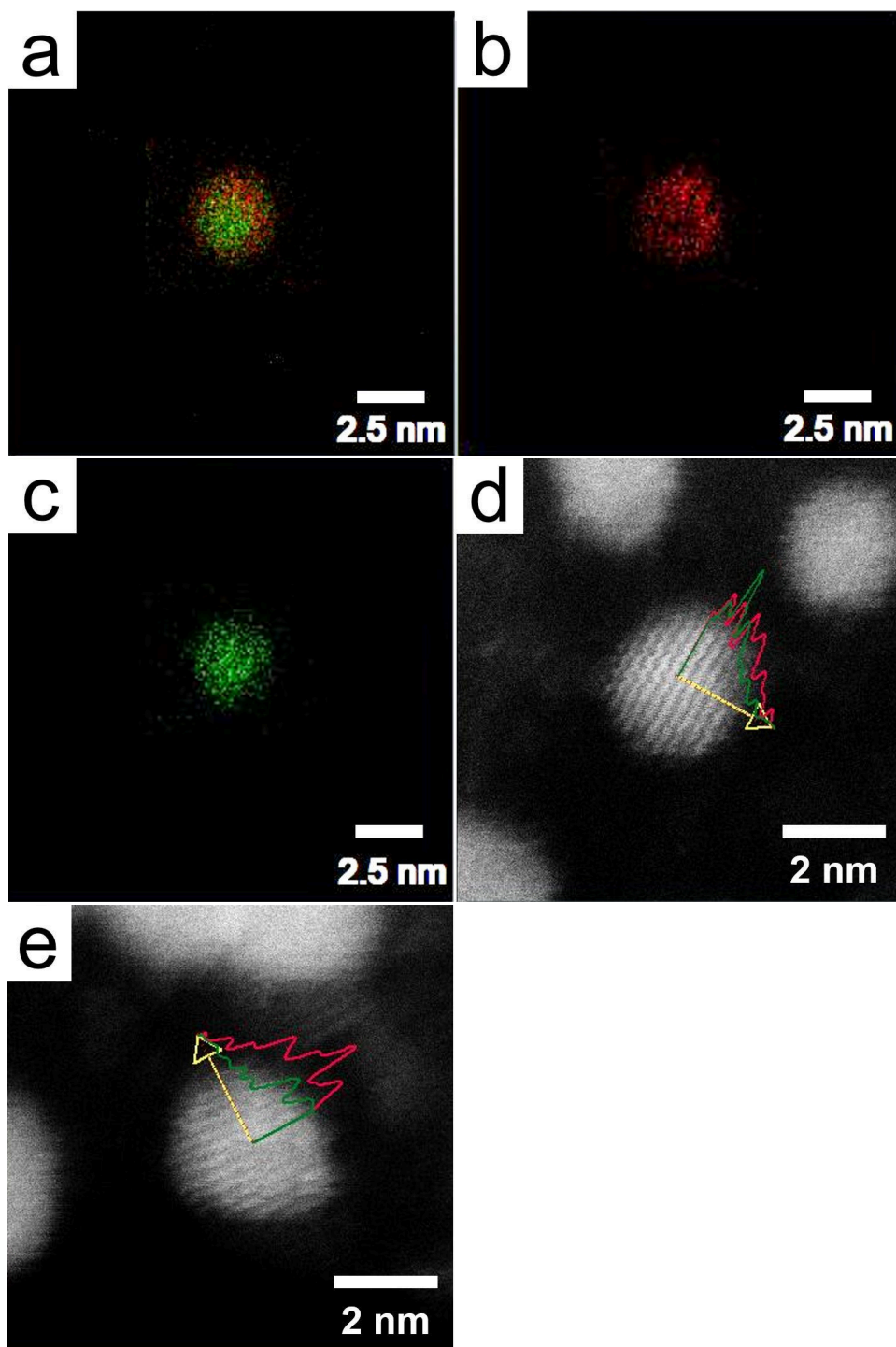


Figure S8. EDS for AuPt DENs prepared using 5 HT pulses. (a) Overlaid Pt (red) and Au (green) EDS maps. Individual (b) Pt and (c) Au maps of the combined map shown in frame (a). (d) acSTEM line scan of a representative NP. Pt dominates the first ~ 0.6 nm

of the NP, which corresponds to the first two atomic columns (or MLs). This result is consistent with the XPS data (Figure 3). Beyond ~ 0.6 nm, Pt and Au appear to be mixed. (e) acSTEM line scan demonstrating variation in Pt shell thickness. Based on eight line scans, the average Pt thickness on either side of the Au NP core is 0.6 ± 0.2 nm (adding ~ 1.2 nm of Pt to the original Au NP diameter).

Table S3. Electrochemical surface characterization after 20 FAO cycles. Pt coverage (θ_{Pt}) was calculated as $(1 - (Au_f \text{ ECSA}/Au_i \text{ ECSA}))$, using the Au_f ECSA values after catalysis (*vide infra*) and the Au_i ECSA values from Table S1. The $\Delta\theta_{Pt}$ represents the magnitude of the change in θ_{Pt} after catalysis. In other words, it is the difference in the values of θ_{Pt} before catalysis (Table 1; main text) and after the 20th FAO cycle (*vide infra*). The Au_f and Pt ECSAs below were determined by recording surface characterization CVs after catalysis and using the same calculation method as in Table S1. The units for all of the ECSAs below are cm^2 . Surface characterization was performed in N_2 -purged 0.10 M HClO_4 , using the same scan parameters as the CVs in Figure 2a of the main text.

Pulses	θ_{Pt}	$\Delta\theta_{Pt}$	Au_f ECSA	Pt ECSA	$ECSA_{tot}$
1	0.31(3)	0.26(3)	0.18(1)	0.097(8)	0.28(1)
3	0.53(5)	0.30(4)	0.117(6)	0.24(3)	0.36(4)
5	0.68(1)	0.23(1)	0.084(6)	0.43(8)	0.51(8)
10	0.94(1)	0.03(1)	0.016(2)	0.7(2)	0.7(2)

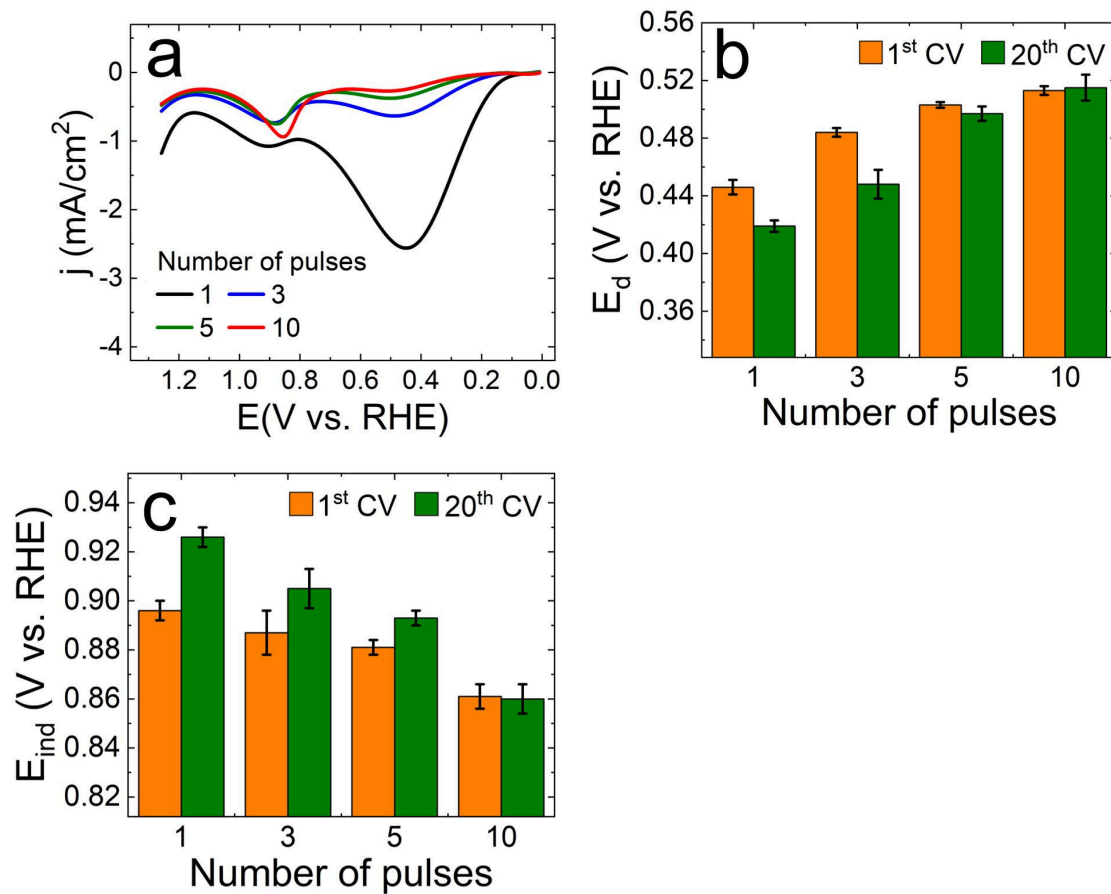


Figure S9. Comparison of FAO results for the forward-going scans of the first and 20th FAO CVs. (a) The forward-going scan of the first FAO CV. Comparison of (b) E_d and (c) (E_{ind}) for the forward-going scans of the first and 20th FAO CVs.

References

1. S. Trasatti and O. A. Petrii, Real surface area measurements in electrochemistry, *Pure Appl. Chem.*, 1991, **63**, 711–734.
2. A. H. Larsen, J. J. Mortensen, J. Blomqvist, I. E. Castelli, R. Christensen, M. Dulak, J. Friis, M. N. Groves, B. Hammer and C. Hargus, The atomic simulation environment—a Python library for working with atoms, *J. Phys. Condens. Matter*, 2017, **29**, 273002.
3. A. S. Lapp, Z. Duan, N. Marcella, L. Luo, A. Genc, J. Ringnalda, A. I. Frenkel, G. Henkelman and R. M. Crooks, Experimental and Theoretical Structural Investigation of AuPt Nanoparticles Synthesized Using a Direct Electrochemical Method, *J. Am. Chem. Soc.*, 2018, **140**, 6249–6259.